CHAPTER II

THEORY

2.1 Quantum Dots

2.1.1 Introduction

When the size of a semiconductor crystal is reduced to the nanometer scale with an order of the carrier's de Broglie wavelength, and when the crystal is surrounded by other crystals acting as potential barriers, the freedom of carrier movement is limited. Carriers in a bulk semiconductor which is a three dimensional (3D) structure are free to move in every direction. In other words, they have three degrees of freedom (three DOF). In a quantum well (QW), they can only move in a plane (two DOF). While shrinking another dimension leads to a quantum wire (QWR) structure, where only movement in one direction is allowed (one DOF). Carriers in a quantum dot are completely confined or in all three dimensions. The electronic structure is analyzed in the terms of the density of electron states (DOS). The density of states (DOS) changes from a continue distribution to a discrete one in a QD. The DOS consists of a series of sharp (delta-function like) peaks corresponding to the discrete eigen-energies of the electrons. Because of their discrete energy levels, much like an atom, they are sometimes called "artificial atoms". The energy levels and the spacing of discrete electron level depend on crystal size and shape of the QD, and the depth of the potential.

QDs have not only been found important applications in existing semiconductor devices, but they also have a great potential for future quantum functional devices. For the optimization of existing devices a better control of size, shape, and density of large ensembles of nanostructures has been a significant research topic for the last few years and is still progressing. For examples, lasers with ultra-low threshold currents and high temperature stability have been predicted and realized as well as high-speed optoelectronic devices have been realized [8]. Moreover, QDs have attracted much attention for research areas which have their origin in atom physics, such as quantum optics and quantum

หอสมุดกลาง ศูนย์วิทยทรัพยากร
จุฬาลงกรณ์มหาวิทยาลัย

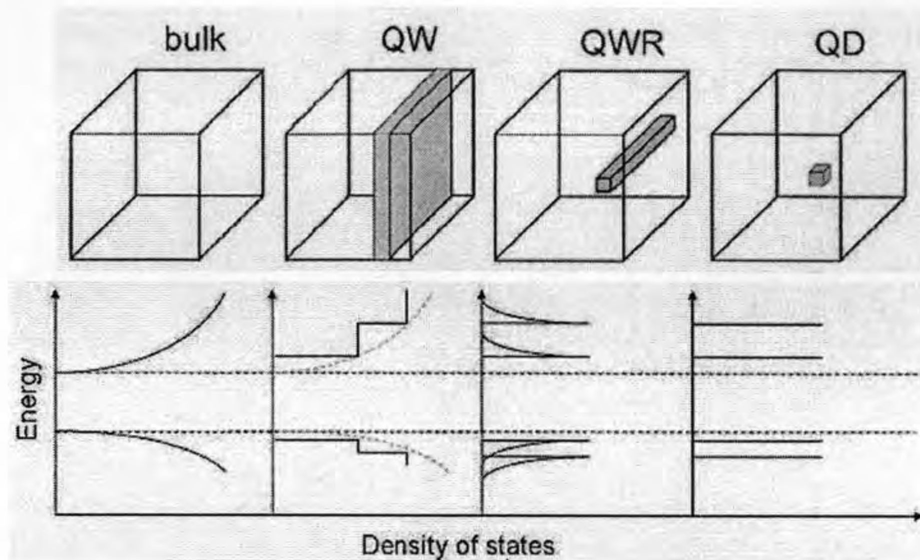

Figure 2.1: Density of states for semiconductor structures for different degrees of confinement

information processing.

Semiconductor quantum dots can be fabricated or grown using different techniques, such lateral patterning of a QW structure performed with e-beam lithography and reactive ion or wet etching (eg. vertical quantum dot from AlGaAs/InGaAs/AlGaAs double barrier heterostructure), intermixing by focused laser beams or focused ion beams (eg. silicon nanocrystals), chemical synthesis (eg. CdSe and ZnSe nanocrystals), natural formation at the interfaces of a QW and Stranski-Krastanov self-assembled epitaxial growth (eg. InAs and InP QDs). Among all of fabrication techniques, self-assembly leads to the formation of defect-free QDs which provide good optical and electrical properties.

2.1.2 Quantum Dots Fabrication by Stranski-Krastanov Growth Mode

In the case of lattice-matched epitaxy, the epitaxial growth generally proceeds in atomic layer-by-layer (Frank Van de Merwe growth mode). In some growth conditions, 3D islands are formed at the beginning of the growth (Volmer-Weber growth mode). The Stranski-Krastanov growth mode is used in this work. The growth of 3D islands are formed after the completion of a few complete layers. The mechanism is based on the thermodynamic instability during the deposition of an epitaxial film on a lattice mismatched substrate. A layer of material with a lower band gap and a larger lattice

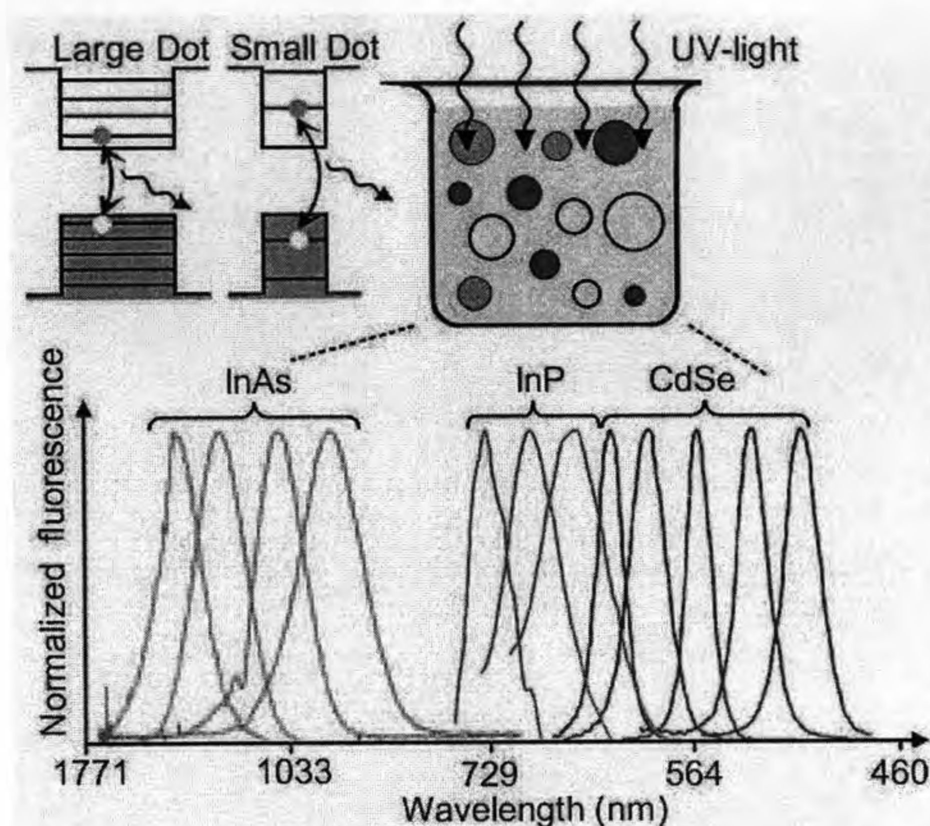

Figure 2.2: Size- and material-dependent emission spectra of several surfactant-coated semiconductor nanocrystal QDs (NCQDs) in a variety of sizes. The blue series represents CdSe NCQDs with diameters of 2.1, 2.4, 3.1, 3.6, and 4.6 nm (from left to right). The green series is of InP NCQDs with diameters of 3.0, 3.5, and 4.6 nm. The red spectral lines are emitted by InAs NCQDs with diameters of 2.8, 3.6, 4.6, and 6.0 nm. Within each color the wavelength is fine tuned by controlling the size of the QDs. The inset shows schematically the dependence of the fluorescence energy on the size of the QD [7].

constant is grown on top of a material with a higher band gap and smaller lattice constant. The various combinations of III-V semiconductors are available. In this study, we focus on the InAs/GaAs system. The lattice mismatch of an InAs layer on top of a GaAs layer is 7%. In the first stage of the growth, below a critical thickness, a pseudomorphic layer with the lateral lattice constant of the substrate is formed. During growth, the elastic energy stored in this layer increases. With increasing thickness, the accumulated compressive strain can no longer be accommodated in a two-dimensional arrangement and the total film energy relaxes through the formation of coherently strained islands on top of the remaining part of the two-dimensional layer, the wetting layer.

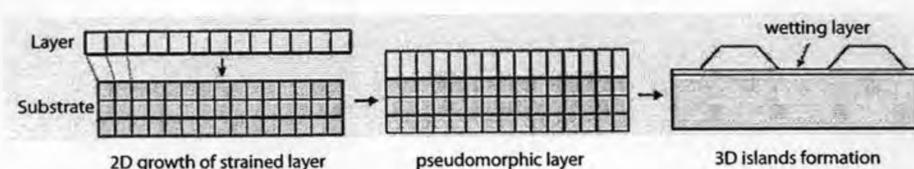

Figure 2.3: The Stranski-Krastanov growth method: the deposition of a lattice mismatched layer on a substrate leads to the formation of a pseudomorphic layer followed by the islands growth [9].

Self-assembled QDs (SAQDs) can be realized by molecular beam epitaxy (MBE) or metal organic chemical vapour deposition (MOCVD) on a variety of different semiconductor material systems, comprising III-V compounds systems and also II-VI and IV-VI materials. Observations by high resolution transmission electron microscopy (TEM) revealed the absence of defects in the islands.

The QD properties, such as size, shape, composition and density, are controllable by the flexibility of the growth conditions and the subsequent capping processes. Solomon et al. demonstrate studies on the influence of substrate temperature, monolayer coverage, group V to III flux ratio, and growth rate for MBE grown InAs and (In,Ga)As QDs with respect to their size and density [10]. This is mainly due to the kinetics of island formation such as surface exchange reactions and diffusion processes. The conditions during overgrowth of the QDs, capping process, also have severe consequences for the QD properties [11]. However, The exact shape, dimension and composition of the self-assembled QDs are generally not known accurately.

2.1.3 Energy Level

Many attempts have been made to calculate the energy levels of quantum dots through complicated numerical models that include realistic shapes and the effects of strain [12, 13, 14, 15]. The results from such models depend heavily on the parameters of the assumed structure. But to gain a qualitative understanding, energy levels are often discussed in terms of the effective mass approximation [16]. Although it is questionable whether this approximation is valid for structures with sharp discontinuities, this approach provides useful intuition and is commonly used.

The simplest model of a QD is the problem of a particle in a infinite barrier.

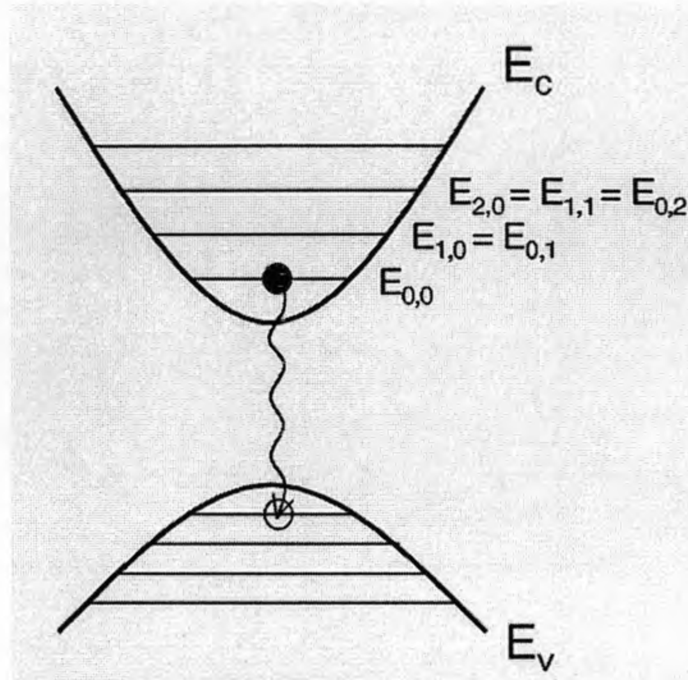

Figure 2.4: Schematic energy diagram of a quantum dot approximated as a harmonic potential, having equally-spaced energy levels. A radiative transition from the lowest level in the conduction band to the highest level in the valence band is indicated.

Consider a single electron in the conduction band of a periodic semiconductor, and ignore spin. For a plane wave with momentum $\mathbf{k}$, we can write its wavefunction as

$$\psi_e(\mathbf{r}) = e^{i\mathbf{k}\cdot\mathbf{r}} u_{e,\mathbf{k}}(\mathbf{r}), \tag{2.1}$$

where $u_{e,\mathbf{k}}(\mathbf{r})$ is periodic: $u_{e,\mathbf{k}}(\mathbf{r}+\mathbf{R}) = u_{e,\mathbf{k}}(\mathbf{r})$, where $\mathbf{R}$ is any lattice vector. In the effective mass approximation, the wavefunction of an electron that experiences a slowly varying potential in a direct-gap semiconductor is approximated as,

$$\psi_e(\mathbf{r}) = f(\mathbf{r}) u_{e,\mathbf{0}}(\mathbf{r}), \tag{2.2}$$

where $f(\mathbf{r})$ is the envelope function, which satisfies Schrödinger's equation:

$$\left\{ -\frac{\hbar^2}{2m^*}\nabla^2 + V(\mathbf{r}) \right\} f(\mathbf{r}) = E f(\mathbf{r}) \tag{2.3}$$

Here, m^* is the effective mass, related to the curvature of the conduction band at $\mathbf{k} = 0$, $V(\mathbf{r})$ is the effective potential, and E is the energy of the state.

Self-assembled InAs quantum dots are highly flattened in the z direction, and it has been reported that the energy-level spacings can be fairly constant. Thus, a commonly

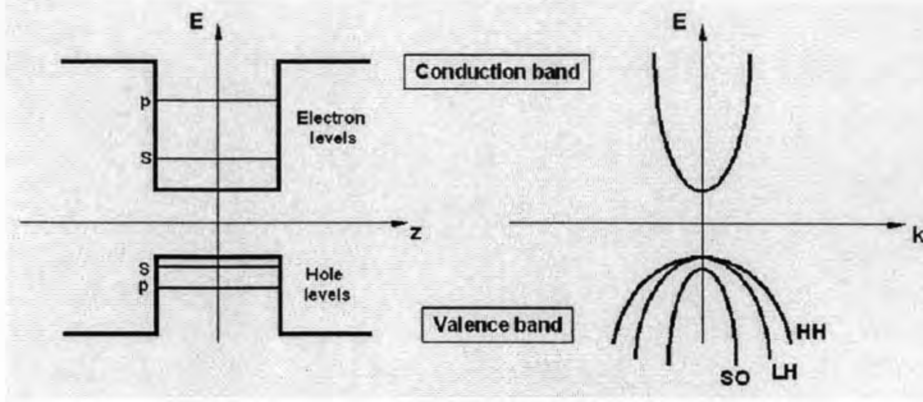

Figure 2.5: Schematic energy diagram for the quantum dot and barrier, and band structure showing the conduction band, heavy hole (HH), light hole (LH) and split-off (SO) bands.

chosen potential for a quantum dot is harmonic in the x and y dimensions, and an infinite square well in the z direction [17]:

$$V(\mathbf{R}) = \begin{cases} \frac{1}{2}m^*\omega_0^2(x^2+y^2) & ; |z| < L/2 \\ +\infty & ; |z| > L/2 \end{cases} \tag{2.4}$$

where L defines the height of the quantum dot, and ω_0 gives the energy-level spacing. The energy levels resulting from this Hamiltonian are [18]

$$E = (n_x + n_y + 1)\hbar\omega_0 + \left(\frac{\pi^2\hbar^2}{2m^*L^2}\right) \tag{2.5}$$

where n_x and n_y are integers ≥ 0, and n_z is an integer ≥ 1. Usually, L is assumed to be small, so that only the $n_z = 1$ states are considered. For InAs quantum dots, the spacing $\omega_0\hbar$ between the lowest two electron energy levels is typically in the range of 30-80 meV. This simple model shows the characteristic quantization of the energy levels due to the confinement and the dependency of the energy levels on the effective masses of the carriers and on the QD size. For holes in the valence bands, the situation is more complicated. There are three bands (heavy-hole, light-hole, split-off) which can mix [16].

First steps towards a more realistic approach are performed by considering the finite height of the confinement potential,the morphological characteristics of the dot (eg. shape and composition) and the influence of strain [12]. The energies of multiparticle states (eg. excitons, multiexcitons) are also included [19, 20].

The dependence on the temperature of energy gap of crystals results from the interaction of the electronic states with the vibrations of the lattice (electron-phonon in-

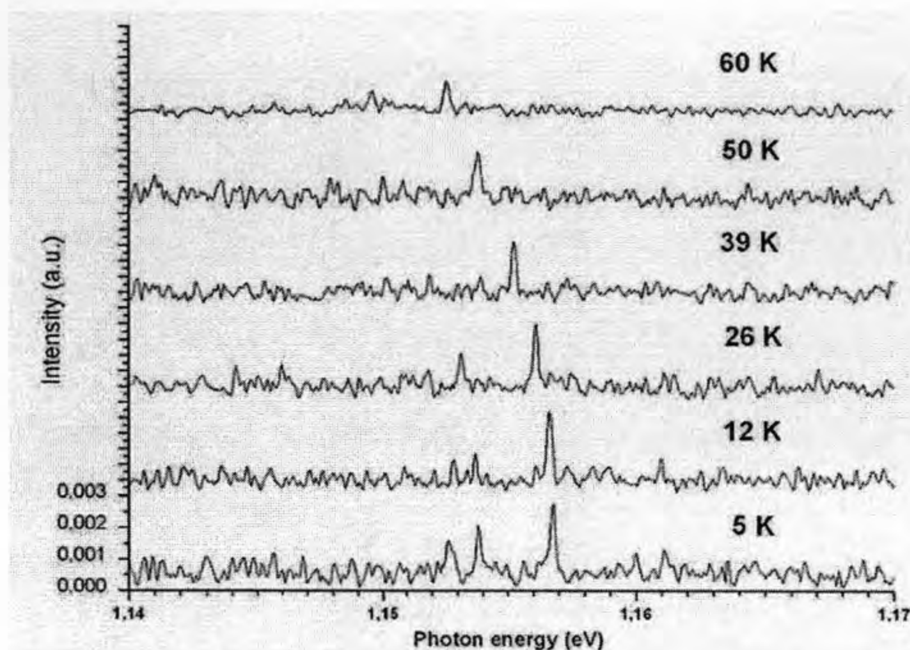

Figure 2.6: Dependence on the temperature of the ground state emission of a single QD [9].

teractions). Transition energies of QDs are thus subject to thermal drift, which is caused by the temperature dependence of the band gaps of the respective semiconductors. The gap shrinkage effect in semiconductors represent a cumulative effect produced partly by electron-phonon interactions and partly by thermal lattice expansion. The first mechanism is usually the dominating one at low temperatures [21]. At high temperatures, both contributions lead to a linear change of the band-gap energy and can have similar magnitude (depending on the material).

2.2 Self-Organized Strain Engineering

The position control of QD sites is mainly pursued by selective overgrowth of prepatterned substrates. Defining QD arrays by patterning is strongly limited by the spatial resolution and accuracy of lithography and pattern transfer. It also introduces additional defects due to the various processing steps and is time consuming. It is possible to overcome these problems by self-organization. The concept is based on self-organized anisotropic strain engineering of strained template layers. The strain is originated from the buried QDs in some thick of spacer layer or from superlattice (SL) layers of mismatch

material.

The magnitude of lattice mismatch is defined as:

$$\frac{\Delta a}{a} = \frac{a - a_0}{a} \tag{2.6}$$

where a_0 and a are the lattice constants of a substrate and epitaxial layer. The epitaxial layer thiner than critical thickness is forced to have the lattice space of in-plane direction (x, y) equal lattice constant of substrate. This force leads to accumulating of strain in epitaxial layer and inducing strain to subsequent layer. Other cases of interactions between mismatch materials also yield strains in both materials.

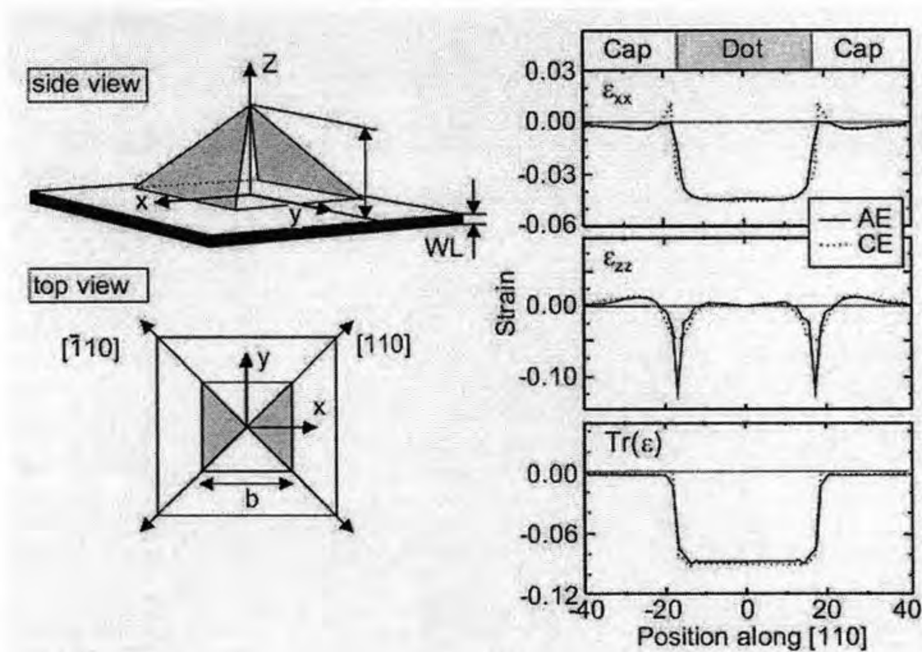

Figure 2.7: Comparison of strain distributions for an InAs QD calculated by AE and CE approximations. Figure (a) describes the model and crystal orientation. Figure (b) shows the diagonal strain components along [110] direction. Solid line corresponds to the AE method and the dashed line to the CE method [22].

The strain distribution in QDs is complicated and has been widely investigated. In this regime, strain calculations can be made using either continuum elasticity (CE) approximation or atomic elasticity (AE) approximation. A comparison of CE and AE calculations of strain fields in InAs QDs is shown in Fig. 2.7. The results agree well except at the edges of the structure. The differences in the calculated band structure modification are also small. The accuracy of the calculation depends critically on the

reliability of the deformation potentials that are needed in calculation of the band edge deformation.

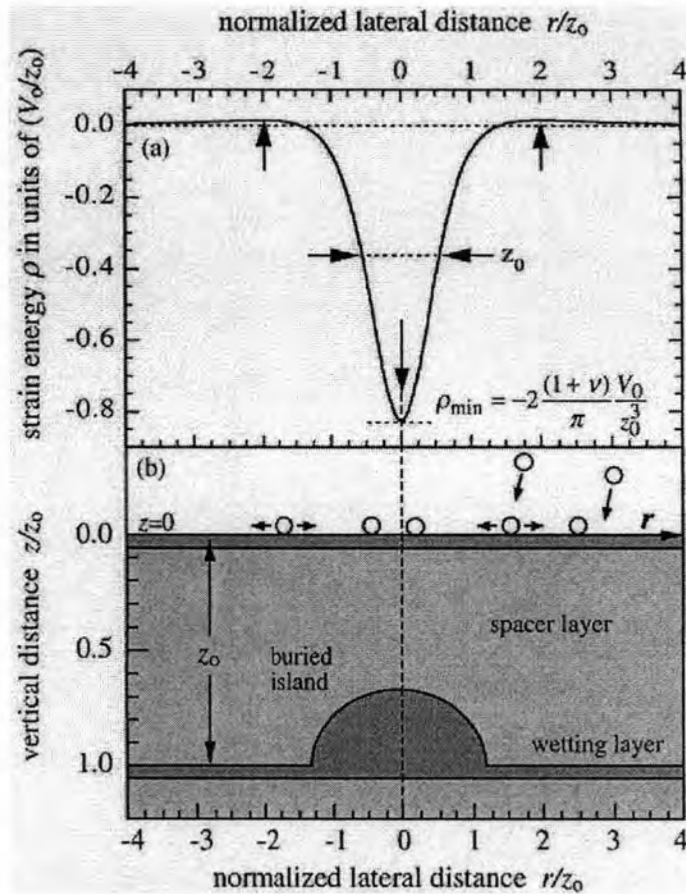

Figure 2.8: Normalized radial strain energy distribution on the wetting layer surface above a buried island in isotropic medium at a depth z_0 by CE model [23].

Buried QDs induce the in-plain strain to capping layer [25]. The strain distribution at the distance of z_0 from the base of QD is shown in Fig. 2.8. The highest tensile strain locate above the centre of buried QDs and give rise to the preferential migration of In adatoms. Hence, vertical alignment of QDs is achieved below a critical GaAs spacer layer thickness as shown in Fig. 2.9.

Several attempts of lateral positioning of QDs are archived by the tailoring strain induced from the layers below to the surface by many growth techniques [26] as well as the utilization of corrugated surface of high-index substrate [27]. The uniform distribution of QD array, control number of quantum dot in QDM and one-dimensional QD chains has been the goals for plenty of investigation as potentials for several quantum devices such as

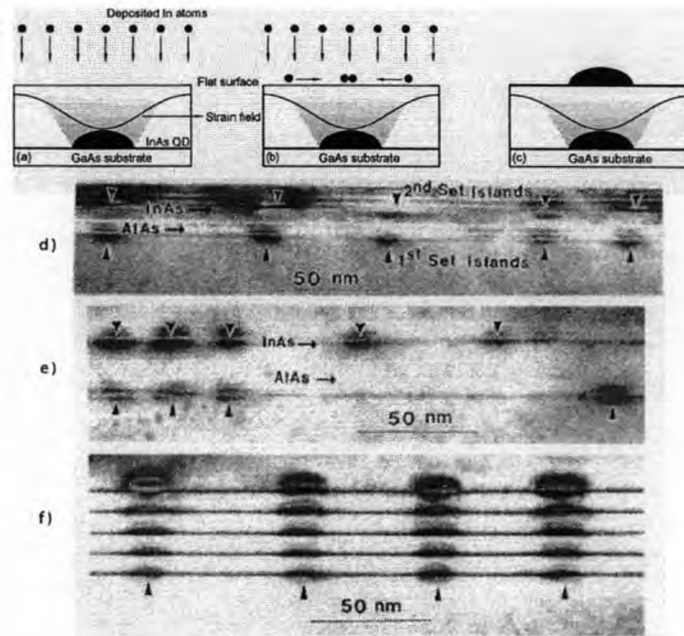

Figure 2.9: The schematic illustration of the vertical alignment process. (a) the uniform In deposition, (b) the accumulation of deposited adatoms at the place where GaAs has high tensile strain (c) the island formation above the buried one. Cross-sectional TEM images of two samples with vertically aligned InAs islands separated by 46 (d) and 92 (e) monolayer thick GaAs spacer layers grown by MBE on GaAs (100) substrates. TEM image of a sample with a stack of 5 vertically aligned islands separated by 36 monolayer thick GaAs spacer layer (f) [24].

quantum memory, quantum cellular automata and quantum information transmission. Our laboratory also develop a kind of lateral positioning control by thin-capping-and-regrowth process which is discussed in chapter 4.

2.3 Optical Anisotropic Property in QDs

Polarization dependence was found both in light emission from QDs and absorption of QDs [28]. The optical anisotropy of QDs was proposed to be arised from asymmetric shape, anisotropic composition and anisotropic strain of QDs [29]. Furthermore, anisotropy of QD structure was enhanced by several techniques, for instance QDs growth at low temperature, QDs growth on misoriented substrate. These structural anisotropy give rise to the difference in the square of the magnitude of the wave vectors in each directions $(\mathbf{k}_x, \mathbf{k}_z, \mathbf{k}_z)$. It results in the anisotropy of optical matrix element $|M|_i^2$ which is defined

as

$$|M|_x^2 = \frac{k_z^2 + k_y^2}{k_x^2 + k_y^2 + k_z^2}\frac{3}{2}|M_b|^2, \tag{2.7}$$

$$|M|_y^2 = \frac{k_z^2 + k_x^2}{k_x^2 + k_y^2 + k_z^2}\frac{3}{2}|M_b|^2, \tag{2.8}$$

where $|M_b|^2$ is the bulk matrix element and degree of optical polarization is

$$DOPA = \frac{|M|_x^2 - |M|_y^2}{|M|_x^2 + |M|_y^2} = \frac{k_x^2 - k_y^2}{k_x^2 + k_y^2 + 2k_z^2} \tag{2.9}$$

Recently, coupling of aligned QDs was introduced that it also contributes to polarization anisotropy [30]. Coupling between QDs leads to degenerate of eigen-energy level and spliting of energy levels. The degree of optical polarization for coupled QDs is

$$DOPA_{\text{coupling}} = \left(\frac{\Delta E_0}{E_1 - E_0}\right) DOPA_{\text{shape anisotropy}} \tag{2.10}$$

where ΔE_0 is the amount of the ground-state energy splitting, E_0 and E_1 are the ground-state and the first excited-state energy levels, respectively, of quantum dot, and $DOPA_{\text{shape anisotropy}}$ is the degree of optical polarization anisotropy arising purely from the shape anisotropy of quantum dot. Equation 2.10 is justifiable as the eigen-energy is related to the wave vector $\mathbf{k}^2$ is directly proportional to the E.